Chapter 4

Result and Discussion

The ratio of glass to agar gel

From the experiments in section 3.3.1 - 3.3.2, the ratio of void volume to weight of glass in the preforms was determined as 30:100 (randomly set glass powder 100 g has a void volume of 30 ml). In contrast to the initial understanding, the volume of void remaining for the agar sol cannot be controlled independently. So, the ratio of glass powder to agar sol is 30 ml of agar sol per 100 g of glass powder. This ratio turned out not to be a free parameter at all. In addition, the experiment showed that if less agar sol was chosen, then the voids between the glass grains were not filled completely. If more agar sol was chosen, the glass segregated leaving a grain-free zone in the upper part of the test tube. Table 4.1 summarizes the results. Until now, it was not possible to keep the grains floating until the sol gelled. But, fortunately, it turned out that the precipitation process did not require a less dense powder packing than the above 30:100 ratio, and that the sintering process did not require a denser packing. So the above ratio was adopted for this thesis work. As

an immediate advantage, the gel preparation route could be set up in the convenient way as described in section 3.3.3.

Table 4.1 Consequences of the variation of the glass powder to agar sol ratio (visual inspection)

ml agar sol per 100 g glass powder	experimental observation
20	agar sol cannot enter all voids
30	all voids filled with agar sol, no segregation
36	segregation
40	segregation

Pre-tests on periodic precipitation

Major experimental effort was devoted to the precipitation tests. This is because until today, no systematic approach to the resulting precipitation patterns is possible, hence the trial and error approach involving a large number of samples. But in this thesis work, the system was used as found in a previous study (28).

Prior to presenting new data, some results from (28) need to be recalled and discussed. In the previous study multilayer precipitates of metal compounds with metal ions Cu could be made in the system of agar gel only. The preferential arrangement of electrolytes was such that the metal ion (Cu) belonged to the outer electrolyte. It was, however, not possible to transfer the agar gel results to particulate silica gels. With the above arrangement of electrolytes, no precipitates occurred at all. Precipitates with periodic features were obtained in systems with the reversed arrangement of electrolytes only, i.e., with the metal ion belonging to the inner electrolyte. Even then, the periodic structure of these precipitates was blurred. No zones distinctly free of precipitate occurred. A typical example is shown in Fig.4.1.

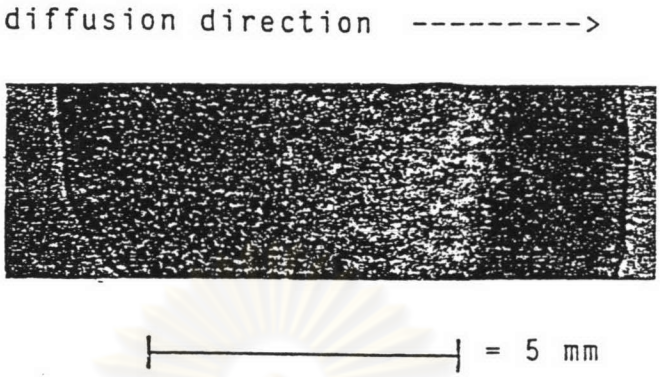

Fig.4.1 Precipitation in the system $Cu(NO_3)_2$-$(NH_4)_2C_2O_4$ in a gel prepared from pyrogenic silica gel with a specific surface area of approx.300 m^2/g (A 300); concentrations of both electrolytes 0.1 mol/l

For reasons of comparison, the entire scope of previous experiments is repeated in this report in table 4.2.

Table 4.2 Solubility situation of performed tests; Ex = outer, In = inner electrolyte; C in mol/l; Q = c(Ex)/c(In); log s = log K_s / [c(Ex).c(In)] ; log $K_s(CuC_2O_4)$ = -7.54 ; log $K_s(FePO_4)$ = -21.89; ■:distinctly periodic precipitate

c (Ex)	C (In)	Q	log s
$Cu(NO_3)_2$ - $(NH_4)_2C_2O_4$ in A200 gel:			
0.1	0.1	1.00	-5.5
0.2	0.1	2.00	-5.8
0.3	0.1	3.00	-6.0
0.5	0.1	5.00	-6.2
0.7	0.1	7.00	-6.4
0.1	0.1	0.50	-5.8
0.2	0.1	1.00	-6.1
0.3	0.1	1.50	-6.3
0.5	0.1	2.50	-6.5
0.7	0.1	3.50	-6.7
0.004	0.0002	20.00	-1.4
0.004	0.0010	4.00	-2.1
0.005	0.0005	10.00	-1.9
0.008	0.0020	4.00	-2.7
0.010	0.0005	20.00	-2.2
0.010	0.0010	10.00	-2.5
0.012	0.0030	4.00	-3.1
0.016	0.0040	4.00	-3.3
0.020	0.0010	20.00	-2.8
0.030	0.0030	10.00	-3.5
0.040	0.0020	20.00	-3.4
0.060	0.0030	20.00	-3.8
$Cu(NO_3)_2$ - $(NH_4)_2C_2O_4$ in A300 gel:			
0.1	0.1	1.00	-5.5
0.1	0.2	0.50	-5.8
$Cu(NO_3)_2$ - $(NH_4)_2C_2O_4$ in agar gel:			
0.1	0.1	1.00	-5.5
0.2	0.1	2.00	-5.8
0.3	0.1	3.00	-6.0
0.5	0.1	5.00	-6.2
$(NH_4)_2C_2O_4$ - $Cu(NO_3)_2$ in A200 gel:			
0.1	0.1	1.00	-5.5
0.2	0.1	2.00	-5.8
0.3	0.1	3.00	-6.0
0.5	0.1	5.00	-6.2
0.7	0.1	7.00	-6.4
0.1	0.2	0.50	-5.8
0.2	0.2	1.00	-6.1
0.3	0.2	1.50	-6.3
0.5	0.2	2.50	-6.5
0.7	0.2	3.50	-6.7

c (Ex)	C (In)	Q	log s
$(NH_4)_2C_2O_4$ - $Cu(NO_3)_2$ in A300 gel:			
0.1	0.1	1.00	-5.5
0.2	0.1	2.00	-5.8
0.2	0.2	1.00	-6.1
0.3	0.2	1.50	-6.3
0.5	0.2	2.50	-6.5
$CuCl_2$ - $(NH_4)_2C_2O_4$ in A200 gel:			
0.1	0.1	1.00	-5.5
0.2	0.1	2.00	-5.8
0.3	0.1	3.00	-6.0
0.5	0.1	5.00	-6.2
0.7	0.1	7.00	-6.4
0.1	0.2	0.50	-5.8
0.2	0.2	1.00	-6.1
0.3	0.2	1.50	-6.3
0.5	0.2	2.50	-6.5
0.7	0.2	3.50	-6.7
$CuCl_2$ - $(NH_4)_2C_2O_4$ in agar gel:			
0.1	0.2	0.50	-5.8
0.2	0.2	1.00	-6.1
0.3	0.2	1.50	-6.3
0.5	0.2	2.50	-6.5
$(NH_4)_2C_2O_4$ - $CuCl_2$ in A200 gel:			
0.1	0.1	1.00	-5.5
0.2	0.1	2.00	-5.8
0.3	0.1	3.00	-6.0
0.5	0.1	5.00	-6.2
0.7	0.1	7.00	-6.4
0.1	0.2	0.50	-5.8
0.2	0.2	1.00	-6.1
0.3	0.2	1.50	-6.3
0.5	0.2	2.50	-6.5
0.7	0.2	3.50	-6.7
$FeCl_3$ - $(NH_4)_3PO_4$ in agar gel:			
0.0001	0.025	0.00	-16.3
0.001	0.025	0.04	-17.3
0.01	0.025	0.40	-18.3
0.02	0.025	0.80	-18.6
0.05	0.025	2.00	-19.0
0.1	0.025	4.00	-19.3
0.2	0.025	8.00	-19.6
0.5	0.025	20.00	-20.0

In this thesis work, the systems of agar gel with untreated glass powder were investigated first. By using the $Cu(NO_3)_2$ as outer electrolyte and $(NH_4)_2C_2O_4$ as inner electrolyte, no precipitation band occured. When changing the arrangement of the electrolyte by using the $Cu(NO_3)_2$ as an inner electrolyte instead of $(NH_4)_2C_2O_4$, a single distinct and dense precipitation band was found. More seriously, precipitates were found only if the metal ion belonged to the inner electrolyte. Thus the problems typical of particulate gels prevailed. A removal of sharp corners and edges from the glass grains by HF acid etching did not result in any improvement. The results are summarized in the upper part of table 4.3 on the following page. The problem is seen in the hydrophilic nature of the glass surface itself, which, like in the particulate silica gels, stems from the ≡ Si-OH groups.

4.1 Pre-tests on periodic precipitation of hydrophobic glass-agar gel system

Silicone oil was chosen to treat the surface of glass powder at first. The systems using hydrophobic glass powder immediately lead to a successful reproduction of the agar gel results. Distinctly periodic precipitates were obtained for both arrangement of electrolytes and for

various concentration conditions. The best results were obtained when the metal ion belonged to the outer electrolyte ($Cu(NO_3)_2$ 0.3 M) and the inner electrolyte was $(NH_4)_2C_2O_4$ 0.1 M. The results are summerized in the lower part of table 4.3. The sketch in Fig.4.2 illustrates the meaning of the symbols s, b, pp and d used to roughly classify the results in table 4.3.

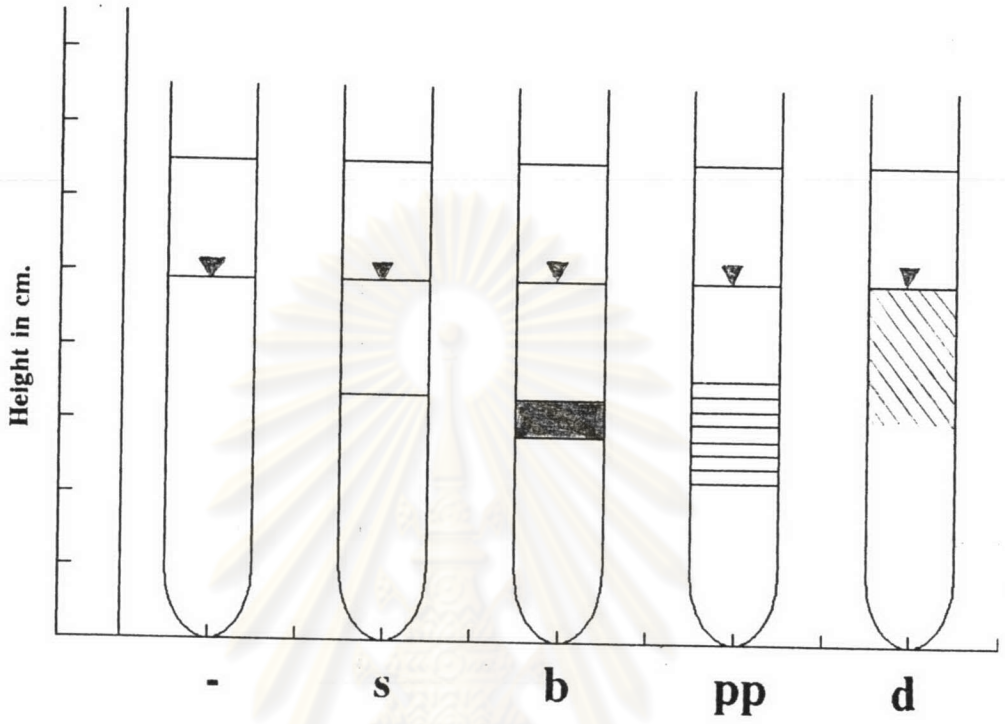

Fig.4.2 Illustration of precipitation patterns typically found in the precipitation experiments summerized in table;

- : no visible precipitate
s : a single distinct and thin layer
b : a distinct and dense precipitation band or zone
pp : distinctly multilayered precipitate
d : diffuse precipitation zone

Table 4.3 Summary of precipitation pre-tests performed for finding the suitable coating and concentration of electrolyte solution

NO. test	C_{out} in M.	C_{in} in M.	glass surface	glass wt.(g)	result	detail
1	$Cu(NO_3)_2$ 0.2	$(NH_4)_2C_2O_4$ 0.1	only agar	-	-	
	0.3	0.1	only agar	-	pp	-
	0.5	0.1	only agar	-	pp	
	1.0	0.1	only agar	-	-	
2	$Cu(NO_3)_2$ 0.3	$(NH_4)_2C_2O_4$ 0.1	phil	8**	d	
	0.5	0.1	phil	8**	d	-
	0.7	0.1	phil	8**	d	
	0.9	0.1	phil	8**	d	
3	$(NH_4)_2C_2O_4$ 0.2	$Cu(NO_3)_2$ 0.2	phil	8**	b	
	0.3	0.2	phil	8**	b	-
	0.5	0.2	phil	8**	b	
4	$(NH_4)_2C_2O_4$ 0.2	$Cu(NO_3)_2$ 0.2	HF, phil	8	b	
	0.3	0.2	HF, phil	8	b	
	0.2	0.2	-	16**	b,s	-
	0.3	0.2	-	16**	b	
	0.3	0.2	HF, phil	16**	b	
5	$Cu(NO_3)_2$ 0.3	$(NH_4)_2C_2O_4$ 0.1	silicone oil, phob	11	pp	
	0.3	0.1	silicone oil, phob	8	pp	
	0.1	0.1	silicone oil, phob	8	s	see
	0.2	0.1	silicone oil, phob	8	pp	fig. 4.3
	0.3	0.1	silicone oil, phob	8	pp	
	0.4	0.1	silicone oil, phob	8	pp	
	0.5	0.1	silicone oil, phob	8	s	
6	$Cu(NO_3)_2$ 0.05	$(NH_4)_2C_2O_4$ 0.2	silicone oil, phob	8	s	
	0.1	0.2	silicone oil, phob	8	s	see
	0.2	0.2	silicone oil, phob	8	pp	fig. 4.4
	0.3	0.2	silicone oil, phob	8	b	
	0.4	0.2	silicone oil, phob	8	pp	

Table 4.3 (continued Summary of precipitation pre-tests performed for finding the suitable coating and concentration of electrolyte solution

NO. test	C_{out} in M.	C_{in} in M.	glass surface	glass wt.(g)	result	detail
7	$(NH_4)_2C_2O_4$ 0.1	$Cu(NO_3)_2$ 0.1	silicone oil, phob	8	pp	
	0.1	0.2	silicone oil, phob	8	s	see
	0.1	0.3	silicone oil, phob	8	s	fig. 4.6
	0.1	0.4	silicone oil, phob	8	s	
8	$Cu(NO_3)_2$ 0.3	$(NH_4)_2C_2O_4$ 0.1				
		pH 3.5	$(CH_3)_2SiCl_2$, phobe	8	d	
		pH 5.0	$(CH_3)_2SiCl_2$, phobe	8	d	-
		pH 7.3	$(CH_3)_2SiCl_2$, phobe	8	d	
		pH 9.0	$(CH_3)_2SiCl_2$, phobe	8	pp	
9	$Cu(NO_3)_2$ 0.3	$(NH_4)_2C_2O_4$ 0.1				
		pH 3.5	$(CH_3)SiCl_2$, phobe	8	d***	
		pH 5.0	$(CH_3)SiCl_2$, phobe	8	d***	-
		pH 7.3	$(CH_3)SiCl_2$, phobe	8	d***	
		pH 9.0	$(CH_3)SiCl_2$, phobe	8	s***	
10	$Cu(NO_3)_2$ 0.3	$(NH_4)_2C_2O_4$ 0.1	paraffin, phobe	8	pp	see
			$(CH_3)SiCl_2$+ parraffin, phobe	8	pp	fig. 4.8

note: *) gel column had double height ;

**) fraction 63 to 125 μm ;

***) temperature for occuring precipitation is 50°C ;

phil : hydrophilic ;

phobe : hydrophobic ;

the meaning of the symbols s, b, pp, and d is explained in fig. 4.2

Some results from table 4.3 are specified in more detail in Fig.4.3-4.6 on the following four pages. Fig.4.3 and 4.4 illustrates the influence of the outer electrolyte concentration for a series of successful tests. These figures are true quantitative representations of the obtained precipitation patterns. Desirable structures occured in a narrow concentration interval only, and required at least 7 days to develop. It was found that if the concentration of outer electrolyte increased, the distance of the first band from the interface of gel is wider than at lower concentrations. In Fig.4.5, the result is shown that if the concentration of inner electrolyte increases, then the distance of the first band from the interface of gel is shorter than at lower concentration. An explanation in terms of diffusion and supersaturation cannot go beyond the level of mere speculation. This will not be tried in this thesis.

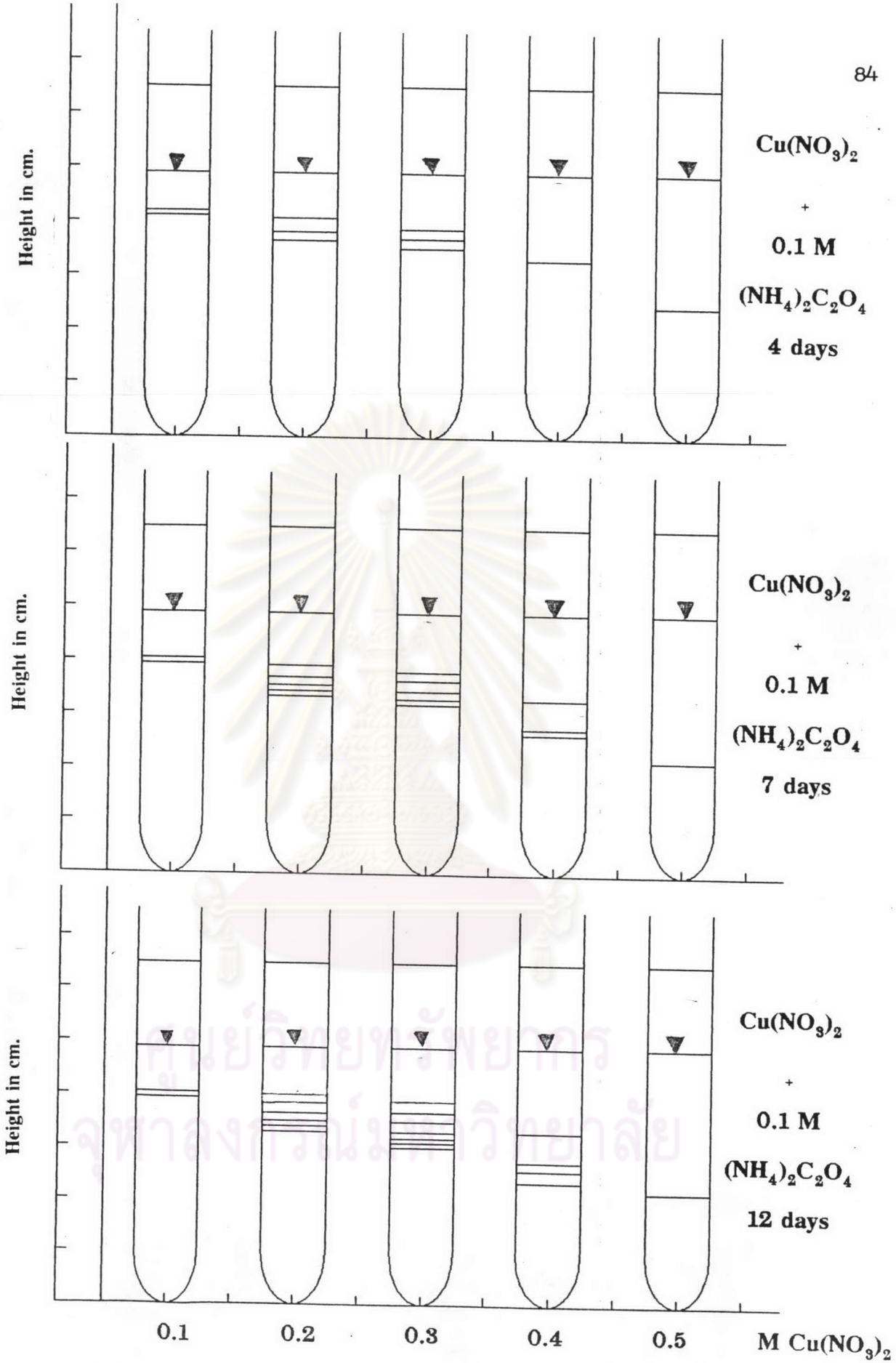

Fig.4.3 Influence of outer electrolyte concentrations on the development of periodic precipitation patterns of CuC_2O_4 in glass powder (silicone oil treated)+agar gel (0.1 M $(NH_4)_2C_2O_4$) system test NO.5

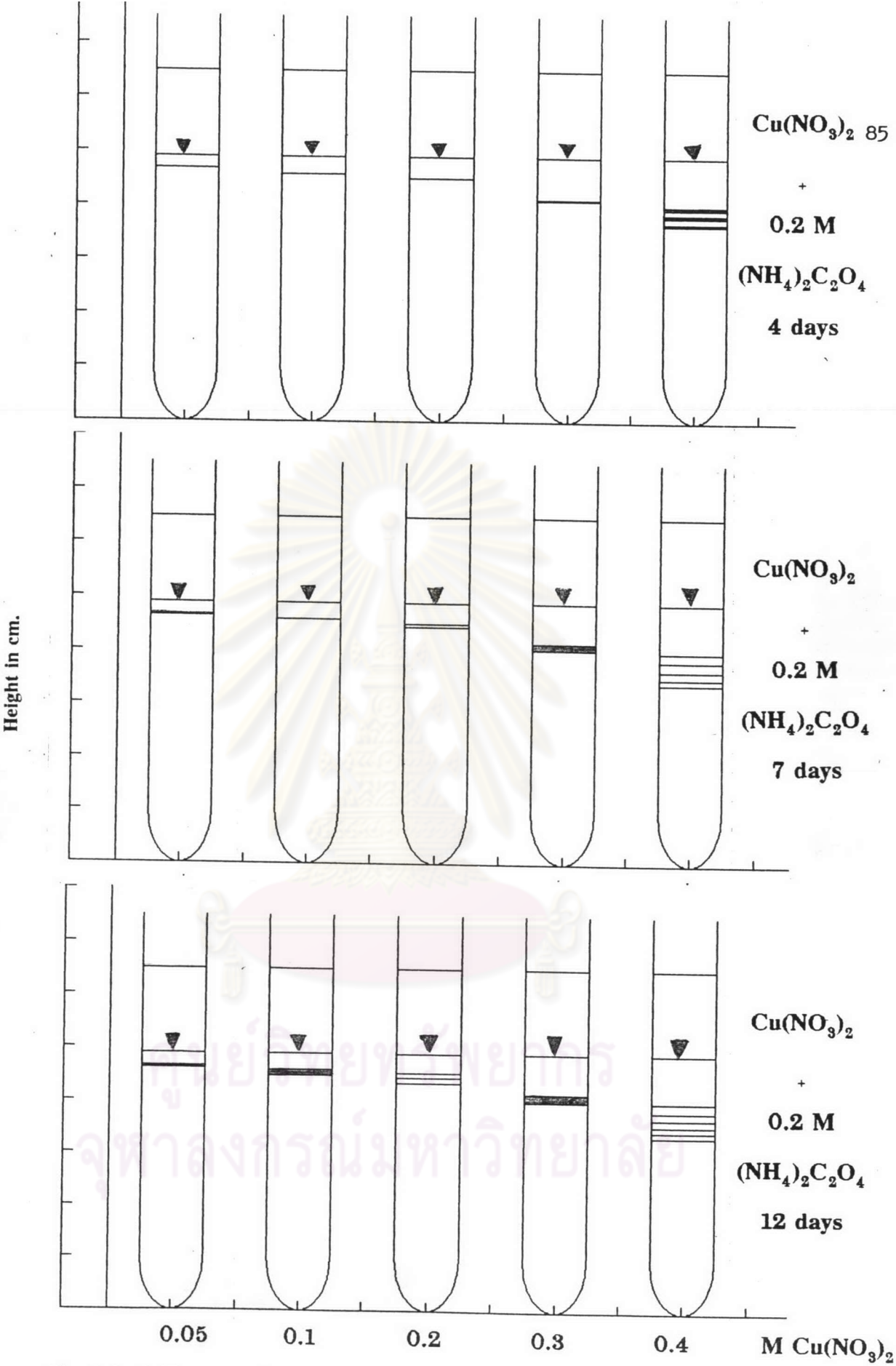

Fig.4.4 Influence of outer electrolyte concentrations on the development of periodic precipitation patterns of CuC_2O_4 in glass powder (silicone oil treated)+agar gel (0.2 M $(NH_4)_2C_2O_4$) system test NO.6

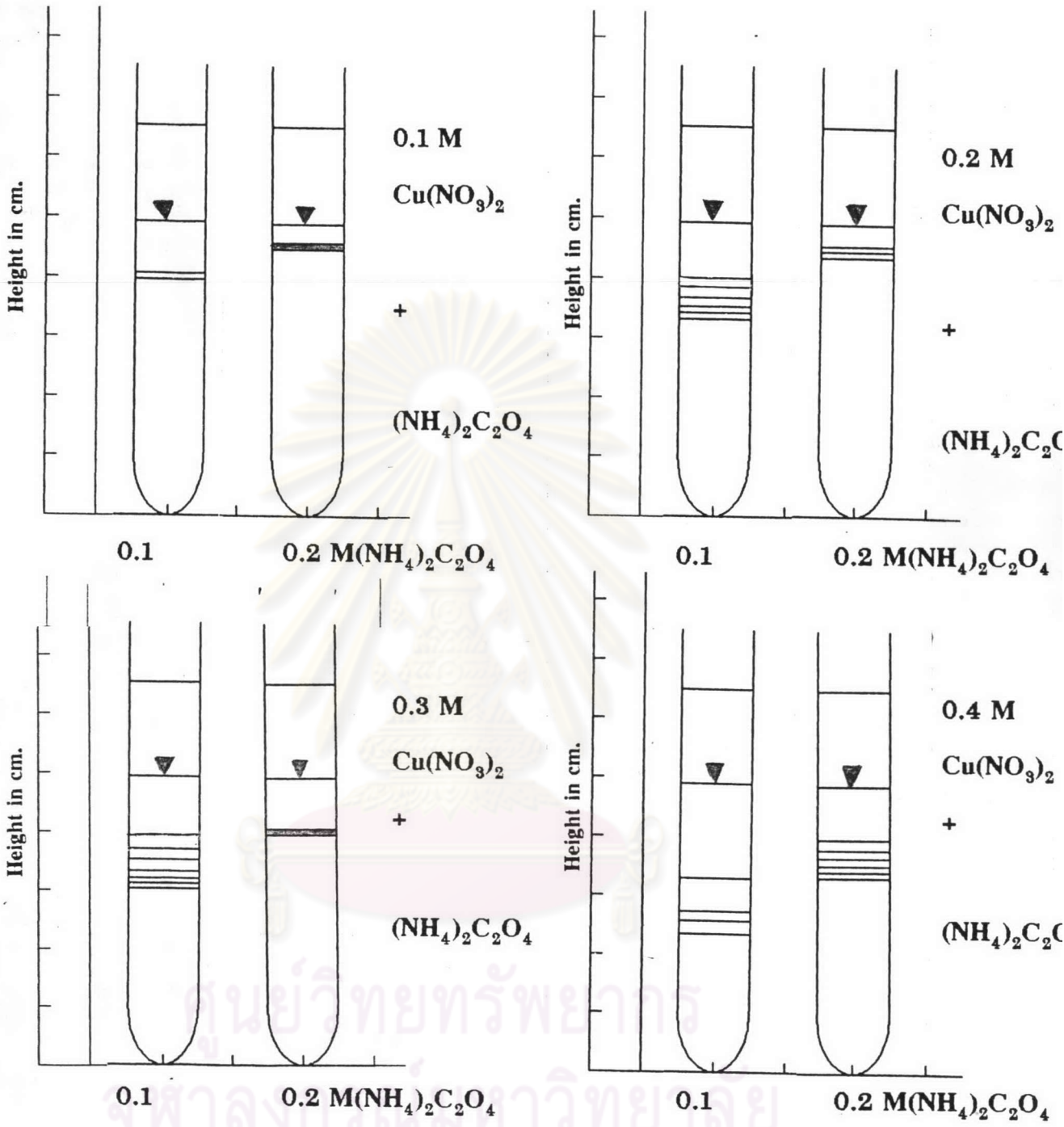

Fig.4.5 Influence of inner electrolyte concentrations of periodic precipitation patterns of CuC_2O_4 in a glass powder (silicone oil treated) + agar gel system (compare test NO.5, 6)

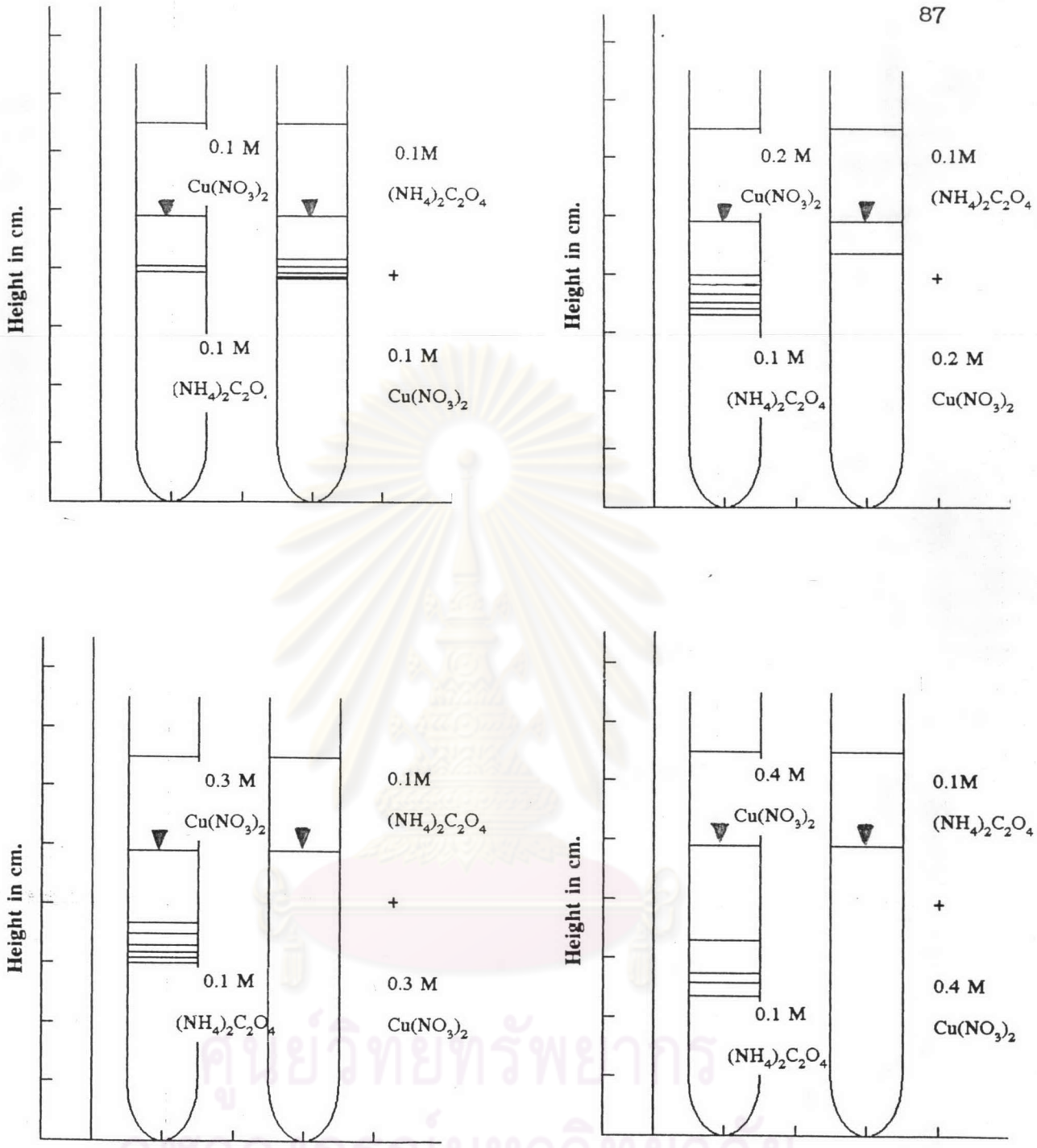

Fig.4.6 Influence of the arrangement of outer and inner electrolyte on the development of periodic precipitation pattern of CuC_2O_4 in a glass powder (silicone oil treated) + agar gel system (test NO.7)

The system of hydrophobic glass treated with silicone oil was very sucessful in generating periodic precipitation. But in the heat treatment step, it caused seriously problems, because the silicone oil impaired the glass property due to its very high reducing power. So an alternative hydrophobic agent was chosen, which is dimethyldichlorosilane ($(CH_3)_2SiCl_2$). The result is not satisfying (see table 4.3). Thus the question occured, why precipitation bands cannot be produced in this case. From direct observation, it was found that the surface of glass treated with silicone oil and dimethyldichlorosilane was different. The particles in the first one were covered with a wrinkled skin while the latter did not differ from the original glass powder. Paraffin wax was studied for its coating effect, too. The pre-tests on periodic precipitates with paraffin coated surfaces were not good because the number of bands was small and the bands were not straight. We assume that the latter problem occured from the non-uniform coating. This was proved by using an optical microscope to characterize the surface of the glass powder. It was found that the coating by paraffin wax was not uniform at all. So, this method of coating had to be improved. This was done by using excess paraffin wax and eliminating the excess by filtation through a filter paper in an oven kept at 80 °C. By this, we

used the low viscosity of molten paraffin to drain off any bulk material of paraffin, leaving behind a thin coating only. The results of the two paraffin coating methods are compared in Fig.4.7. The number of bands or ring was significantly increased by the combined coating with dimethyldichlorosilane and paraffin wax. Fig.4.8 summarizes the influences of all combinations of treatments on the development of periodic precipitation.

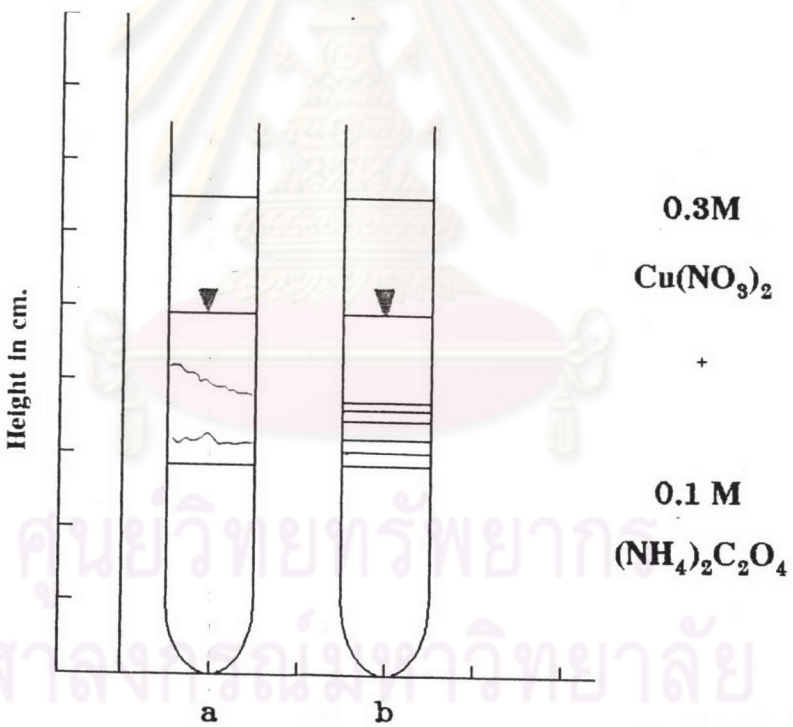

Fig.4.7 Comparison of the periodic precipitation in the glass (coated with paraffin wax) + agar gel system between a) fixed amount of paraffin wax
b) paraffin wax (new method)

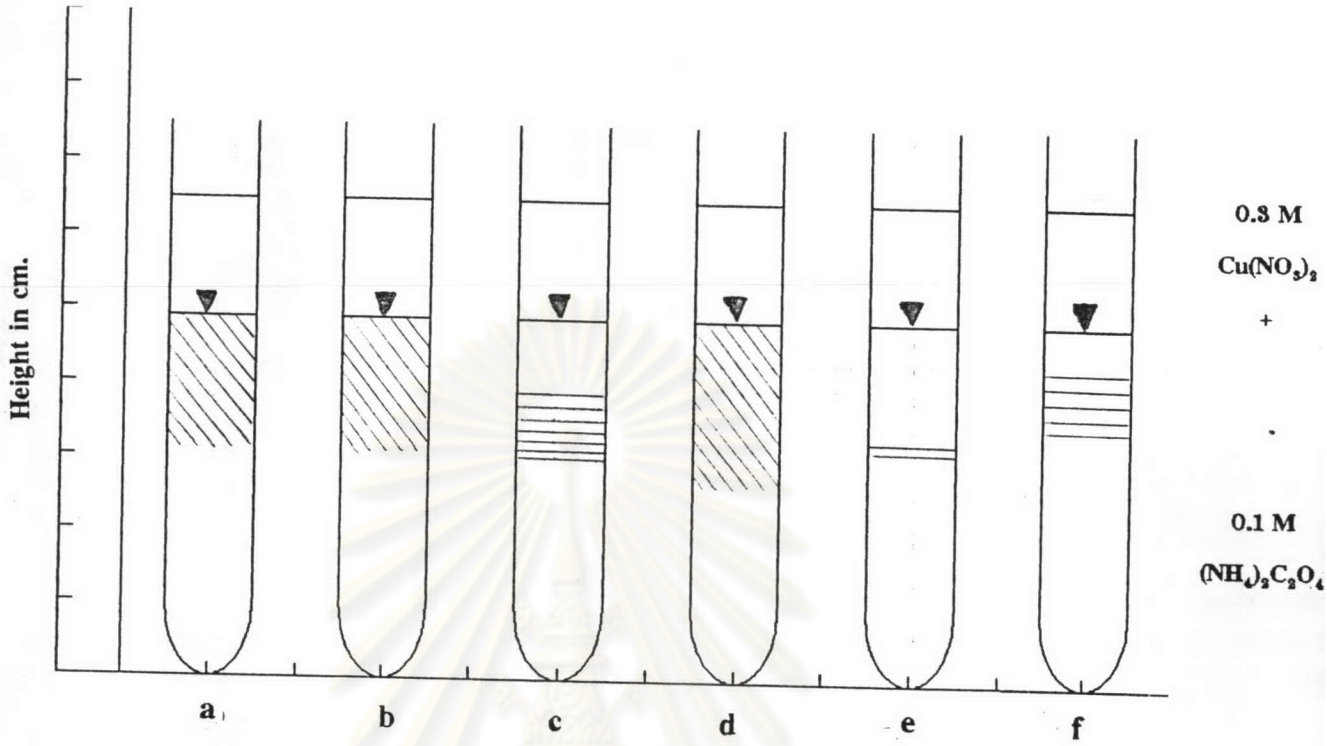

Fig.4.8 Comparison of the influence of each surface treatment on the development of periodic precipitation patterns of CuC_2O_4 in a glass powder + agar gel system

a) not treated

b) treated with HF

c) treated with silicone oil

d) treated with dimethyldichlorosilane $(CH_3)_2SiCl_2$

e) treated with paraffin wax

f) treated with $(CH_3)_2SiCl_2$ + paraffin wax

The characterization of the surface of glass powder by optical microscope is shown in Fig.4.9 - 4.11. Fig.4.9 shows the surface of original glass powder and Fig.4.10 shows the surface of glass powder treated with silicone oil. It is interesting to note that the silicone oil looks similar to Fig.4.11, i.e., the paraffin wax treated sample (improved method). From microscope, we can see that there are two different types of hydrophobic effect. One is due to a chemically bonded molecular layer not visible in the microscope (i.e., the silane), and the other one is due to a physical repellance of water (i.e., by the wrinkled surface of the coating). Silicone oil combines both effects.

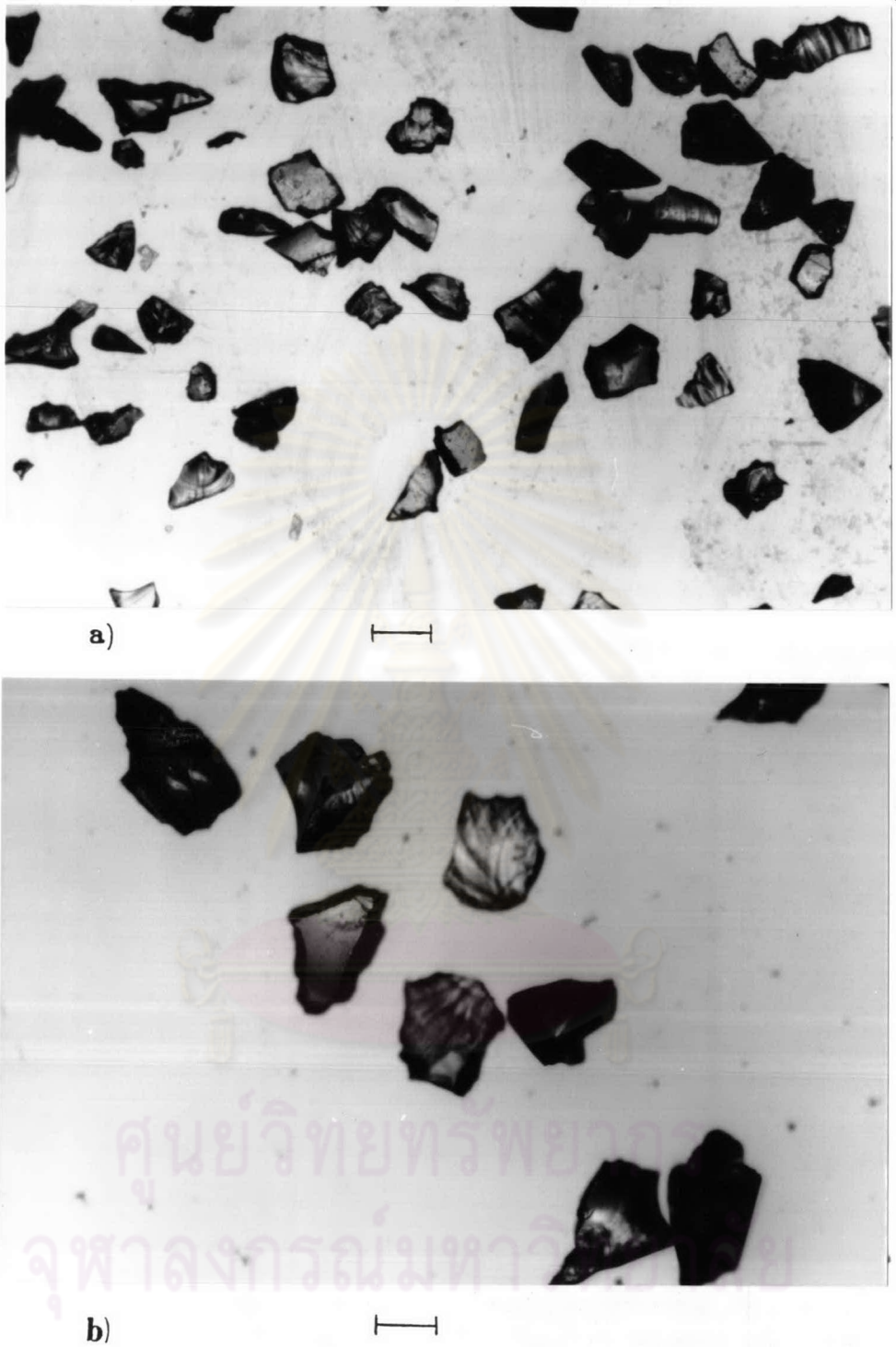

Fig.4.9 Optical micrographs of

a) the original glass powder 63 to 125 μm,

b) the original glass powder 125 to 180 μm,

(bar = 100 μm)

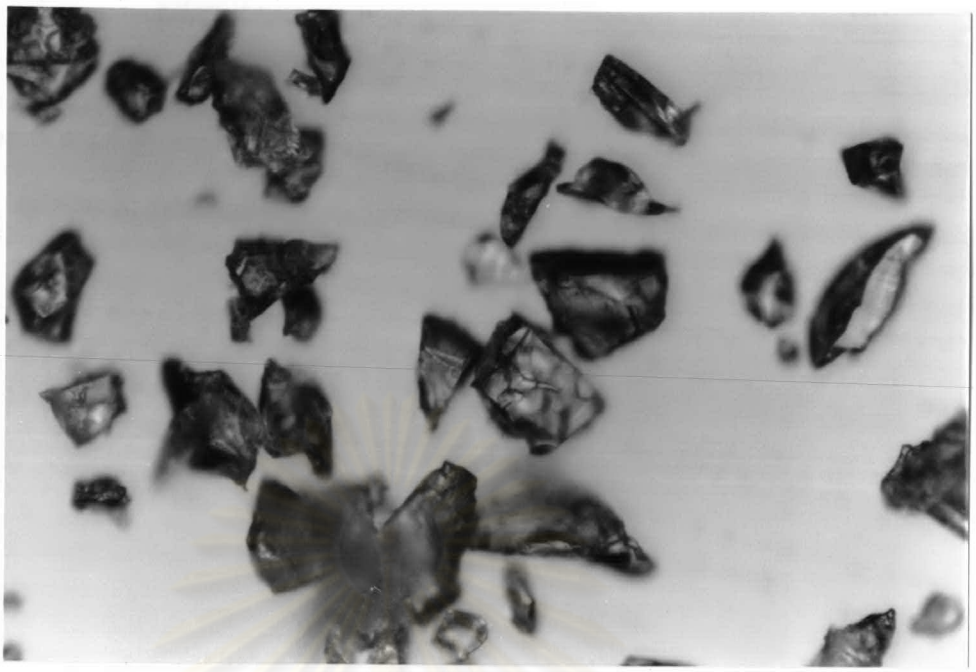

Fig.4.10 Optical micrographs of glass powder 63 to 125 μm, coated with silicone oil (bar = 100 μm)

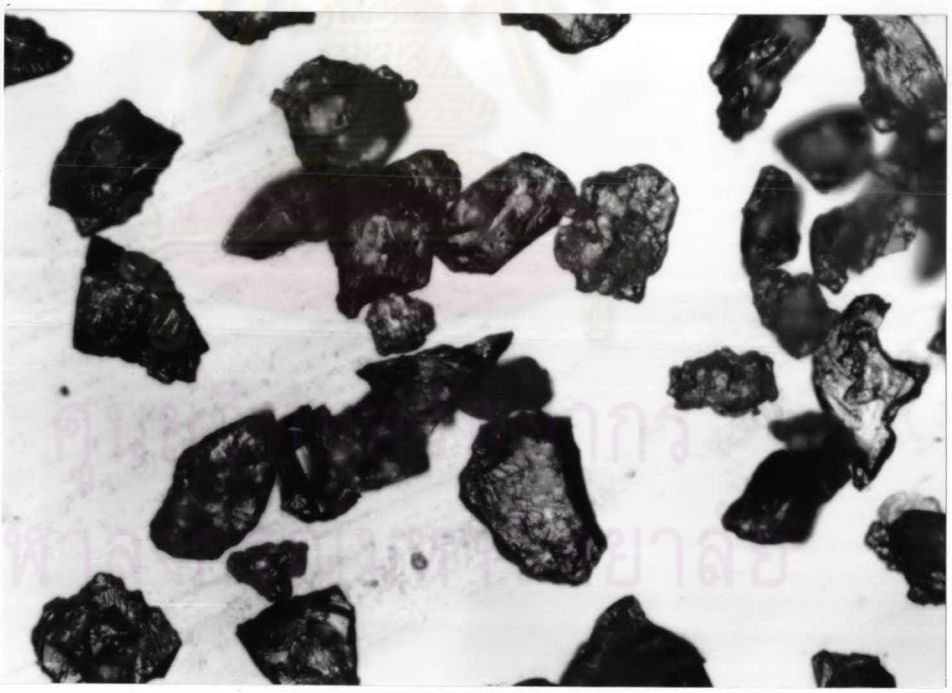

Fig.4.11 Optical micrographs of glass powder 125 to 180 μm, coated with paraffin wax (improved method) (bar = 100 μm)

4.2 Main tests on the periodic precipitation

By the effect of the previously described work, a suitable coating method for the glass surface was found. The glass powder treated with dimethyldichlorosilane and paraffin wax was chosen to be used in the main tests. From experiments in section 3.5, the effects of many additional factors were determined, such as concentration of electrolyte solution (the results are shown in Fig.4.12-4.13), the volume of outer electrolyte (the results are shown in Fig.4.14) of the pH value (the results are shown in Fig.4.15) of the size of tube (the results are shown in Fig.4.16) of the particle size of glass powder (the results are shown in Fig.4.17) and of alternating of temperatures (the results are shown in Fig.4.18). Fig. 4.12-4.14 demonstrate that the desired diversity of precipitation patterns can be produced in the silane + paraffin treated samples. A ratio of outer to inner electrolyte concentration of 3:1 to 2:1 is favourable. Fig.4.15 illustrates that when pH increases, the distance between band is increased too. This is a powerful tool to control band spacing. The cause is not clear, but may be seen from the stability of the precipitates at various pH values. When comparing the solubilitis (18-25^{o}C) of copper (II) axalate and hydroxide (37), log K_S = - 19.66 for $Cu(OH)_2$, log K_S = -7.64 for CuC_2O_4, then it is likely that at increaed pH

valus, the hydroxide is precipitated instead of the oxalate. This is also suggested by the obsevation, that the color of the precipitate changes. From light blue to dark blue. Fig. 4.16 shows that when the diameter of tube is increased, the distance between bands is increased too. Fig.4.17 illustrates that the small size fraction (63 to 125 μm) makes band occur earlier than the big size fraction (125 to 180 μm). Finally, Fig.4.18 shows that the temperature is a very importance factor. At low temperatures, bands were very thick; periodic patterns did not occur. Fig.4.19 illustrates the results for other shapes of preform. It shows that periodic precipitation bands can be produced in other shapes, too. This is of major importance for the further development of functional materials. A rod with a distinct sequence of conductive layers would not yet exhibit any specifically interesting electrical functions. But a piece containing distinct loops of conductive matter definitely would.

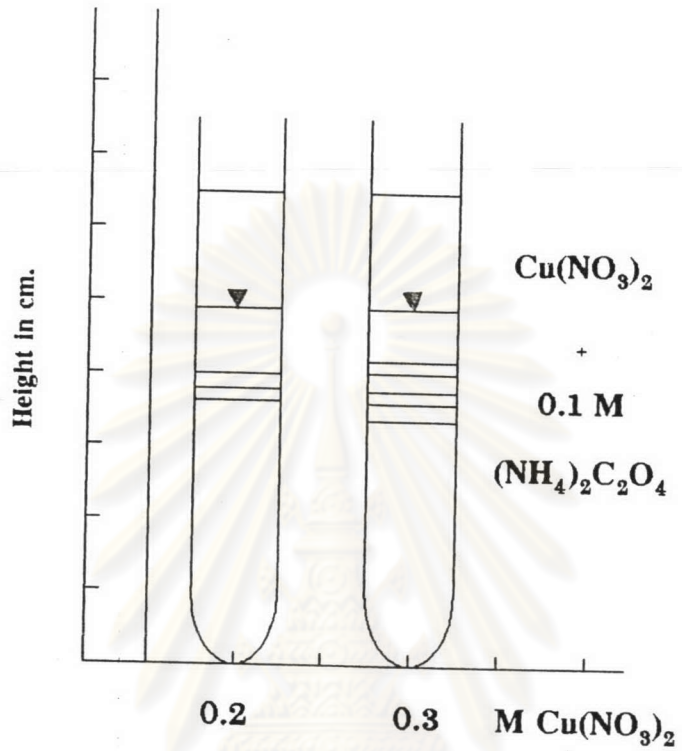

Fig.4.12 Influence of outer electrolyte concentration on the development of periodic precipitation patterns of CuC_2O_4 in a glass powder ($(CH_3)_2SiCl_2$ + paraffin wax treated) + agar gel system at 25±5 °C

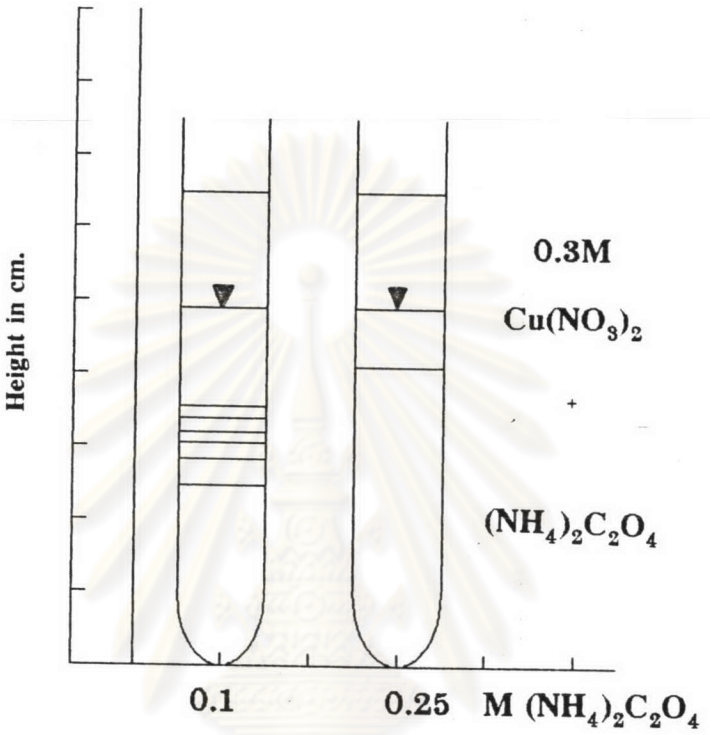

Fig.4.13 Influence of inner electrolyte concentration on the development of periodic precipitation patterns of CuC_2O_4 in a glass powder ($(CH_3)_2SiCl_2$ + paraffin wax treated) + agar gel system at 25±5 °C

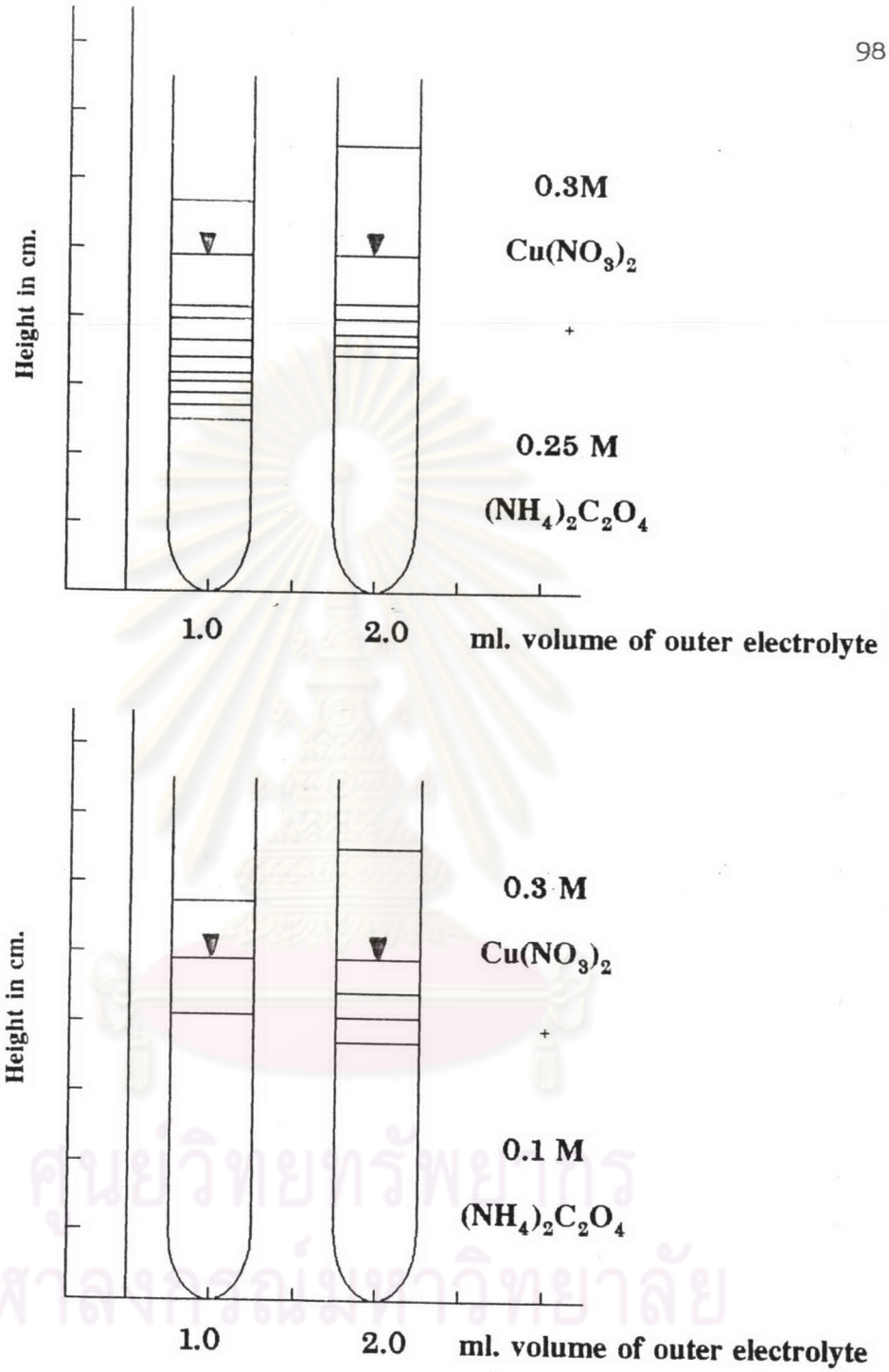

Fig.4.14 Influence of volume of outer electrolyte on the development of periodic precipitation patterns of CuC_2O_4 in a glass powder ($(CH_3)_2SiCl_2$ + paraffin wax treated) + agar gel system at 25±5 °C

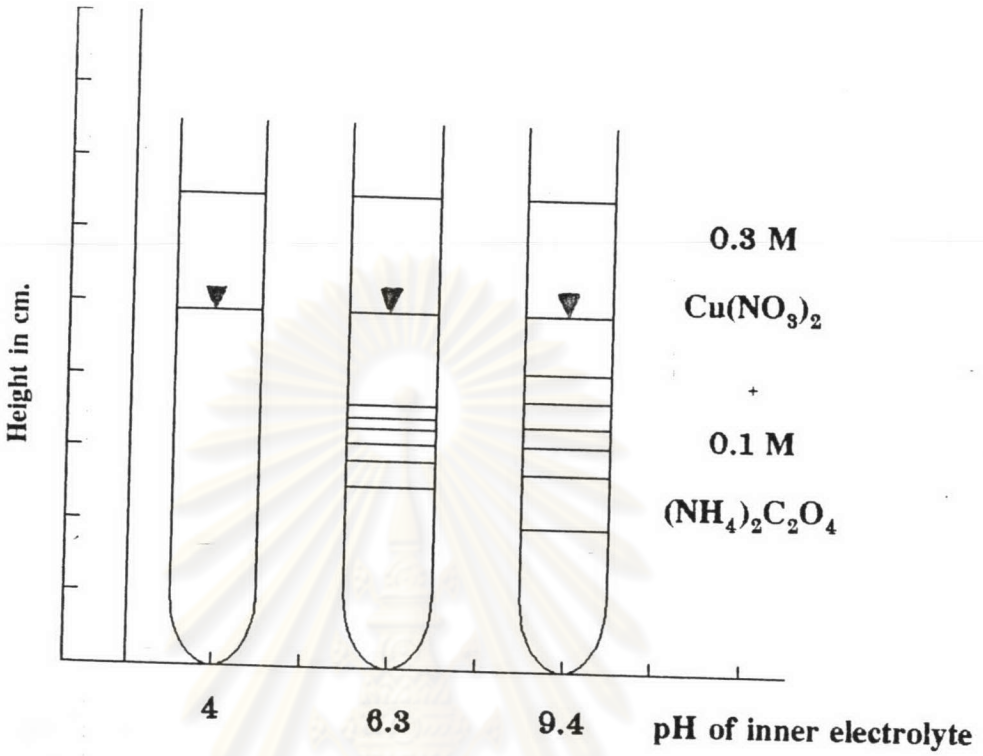

Fig.4.15 Influence of the pH value of inner electrolyte on the development of periodic precipitation patterns of CuC_2O_4 in a glass powder ($(CH_3)_2SiCl_2$ + paraffin wax treated) + agar gel system at 25±5 °C

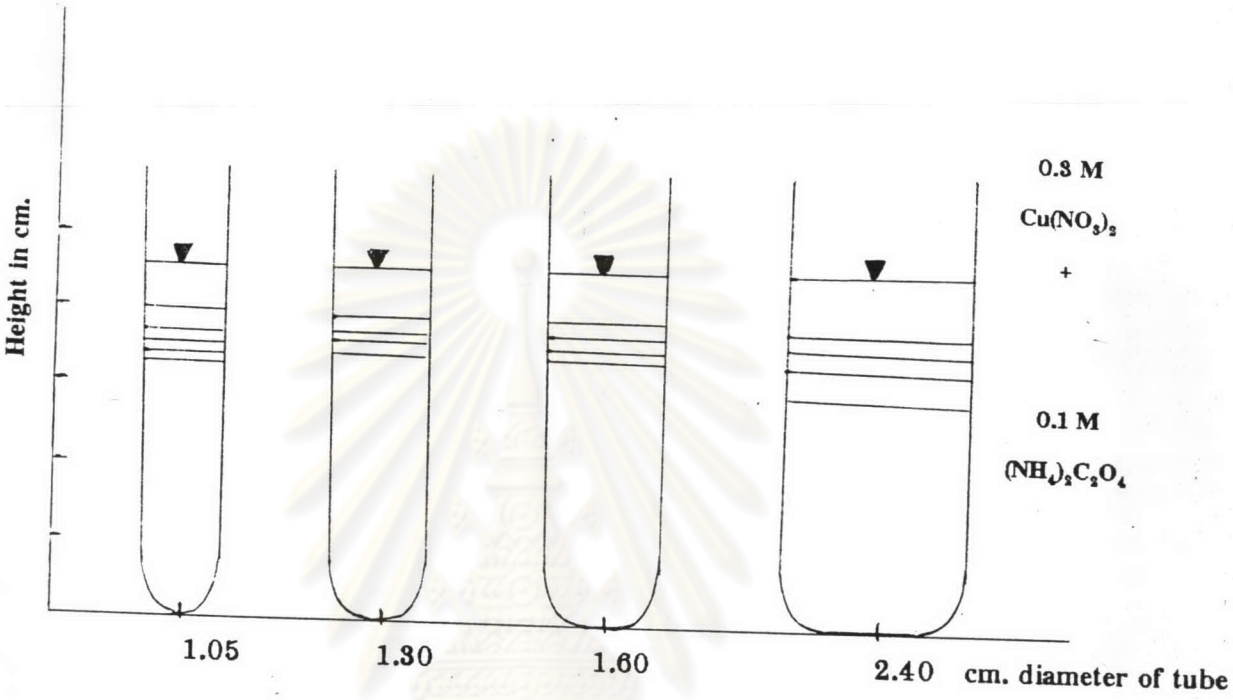

Fig.4.16 Influence of diameter of the tube on the development of periodic precipitation patterns of glass (coated with $(CH_3)_2SiCl_2$ + paraffin wax) + agar gel system at 25±5 °C

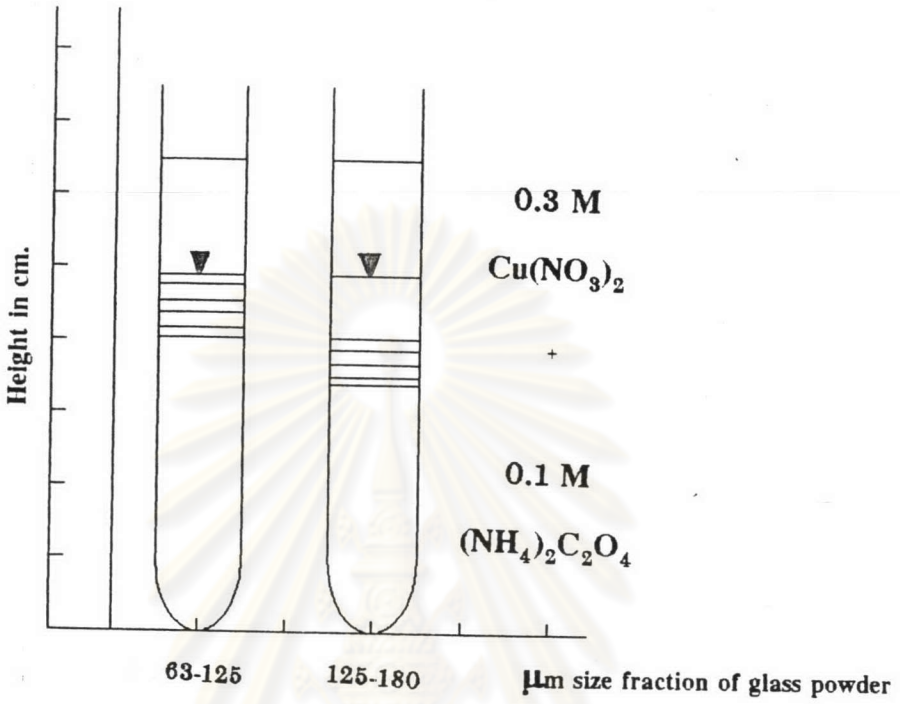

Fig.4.17 Influence of particle size of the glass powder on the development of periodic precipitation patterns of CuC_2O_4 in a glass powder ($(CH_3)_2SiCl_2$ + paraffin wax) + agar gel system at 25±5 °C

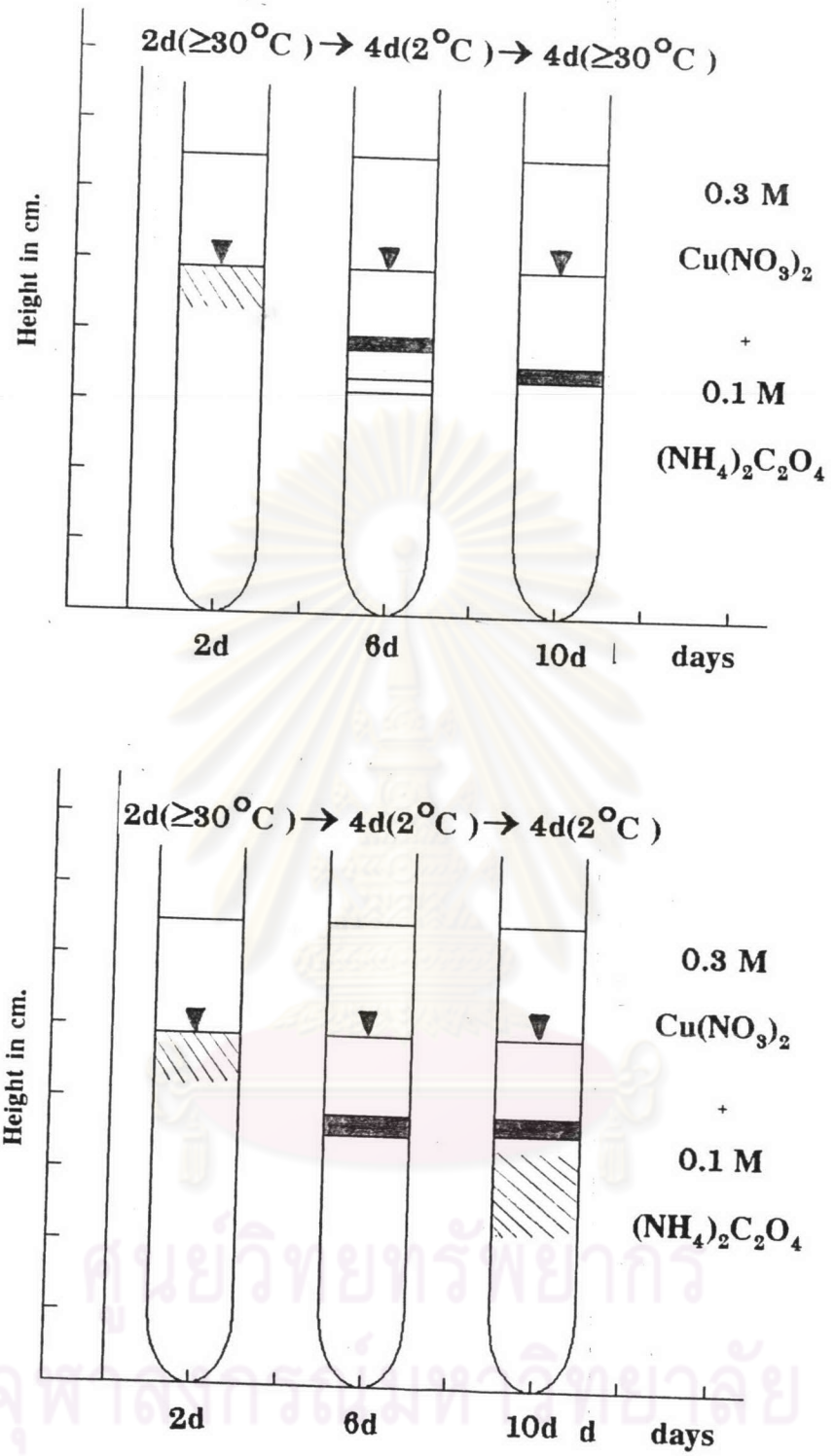

Fig.4.18 Influence of alternating of temperature on the development of periodic precipitation patterns of CuC_2O_4 in a glass powder ($(CH_3)_2SiCl_2$ + paraffin wax treated) + agar gel system

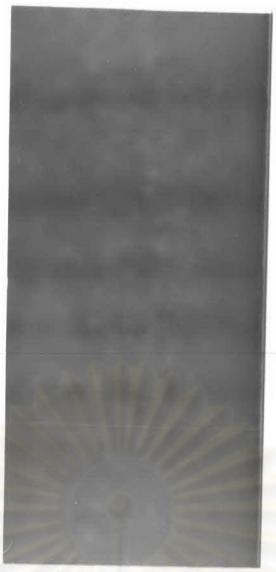

a)

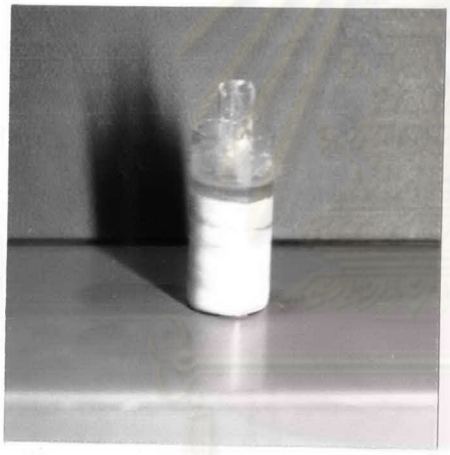

b)

c)

Fig.4.19 Periodic precipitation in tube preform(a), hollow rod preform(b) and torus preform(c) in system of glass (coated with $(CH_3)_2SiCl_2$ + paraffin wax) + agar gel; outer/inner electrolyte concentration = 0.3 M $Cu(NO_3)_2$/0.1 M $(NH_4)_2C_2O_4$

4.3 Pre-test on heat treatment

Samples bound by dried agar gel but not pressed were heat treated at a temperature close to T_L = 724 °C. Some of the samples contained one or more precipitated copper oxalate bands, in one case, a sample with a distinct and dense precipitation zone was used. The samples densified to a translucent glass. Due to the high temperature applied, however, the shape was distorted (see Fig.4.20). Solving this problem is not a task of the present thesis, but is being investigated by a parallel thesis. The tests showed that even dense precipitates can be incorporated in the glass phase without any problems. Beyond this, they suggest that upon careful selection of the temperature,the pressing step might be by-passed. This would mean another significant simplification of the preparation route.

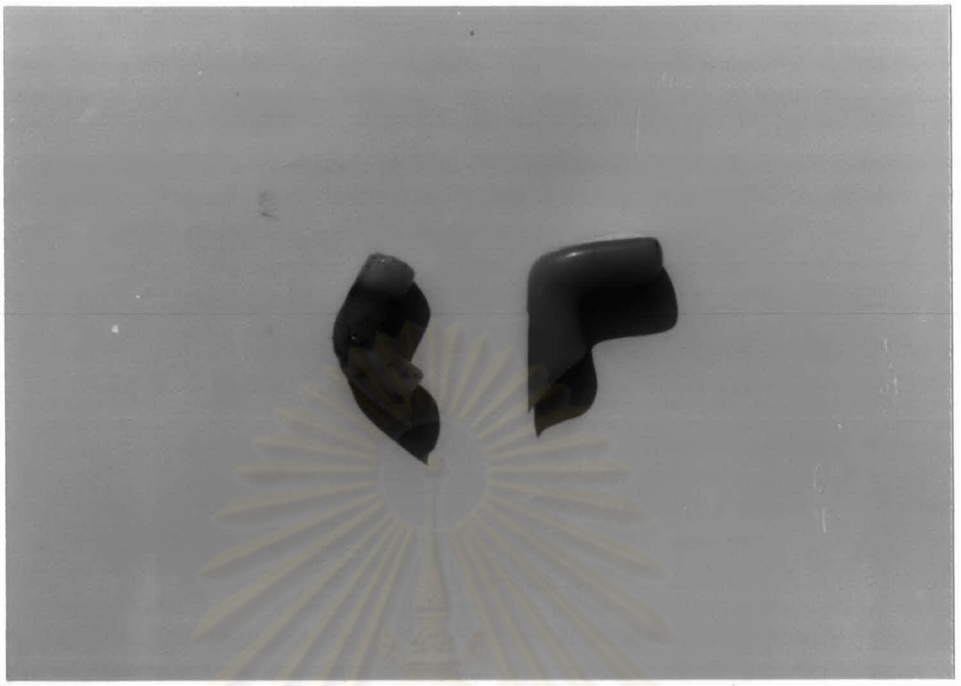

a)

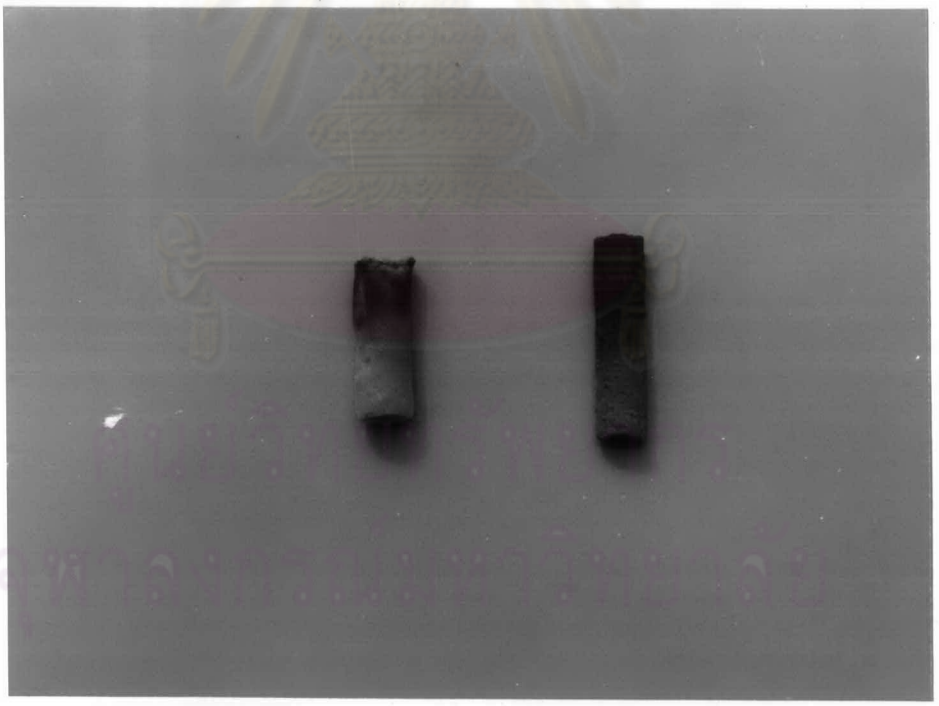

b)

Fig.4.20 The preform of glass + agar gel system, heat treatment at a)700 ^{o}C; left: dense precipitation and aiffuse zone precipitated; right: no precipitation zone. b)550 ^{o}C

Severe problems occurred with samples containing powder surface-treated with silicone oil. The oil had a considerable oxygen deficiency. It decomposed to white SiO_2 at the outside (see Fig.4.21) and to black Si at the inside.

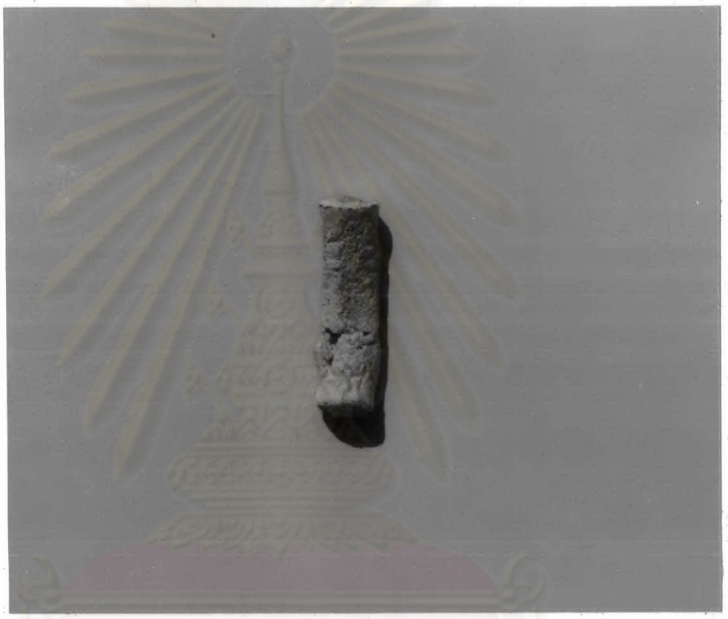

Fig.4.21 Sample preform, surface treated with silicone oil; the oil decomposed to white SiO_2 at the outside

Paraffin wax and dimethyldichlorosilane did not show this problem and was completely decomposed and removed by heat-treatment.

4.4 Microstructure characterization

The microstructure was characterized by optical microscope. The microstructure of a precipitated band prior to heat treatment is given in Fig.4.22 and the heat treated sample is given in Fig.4.23.

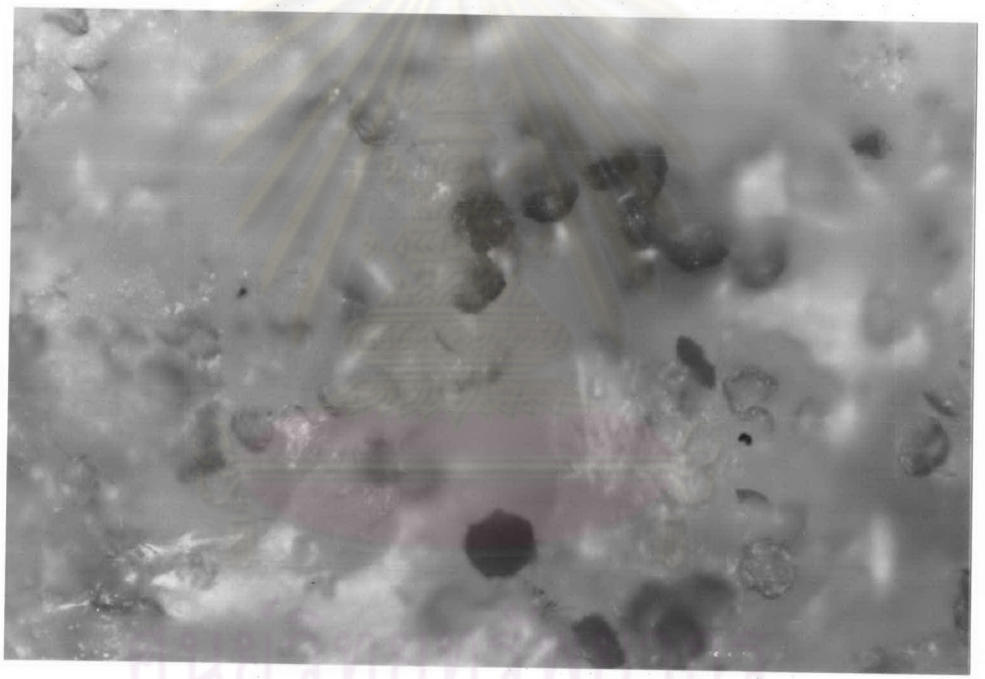

Fig.4.22 The precipitated band prior to heat treatment, optical micrograph
(bar = 100 μm)

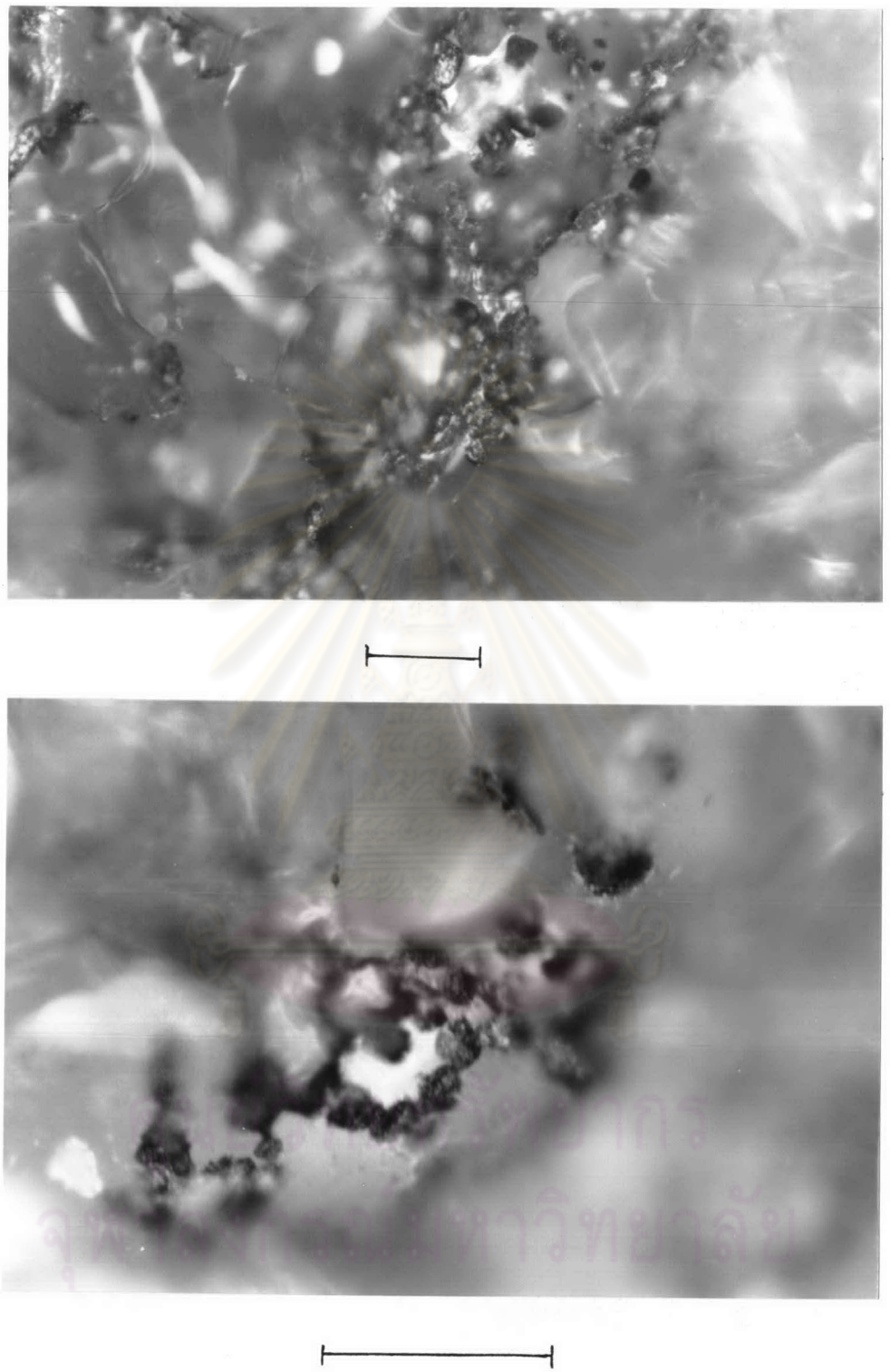

Fig.4.23 Optical micrograph of precipitated band after heat treatment

(bar = 100 μm)

The interfaces of precipitate and glass after heat treatment studied by scanning electron microscope (SEM), is given in Fig.4.24. The white phase is Cu compound.

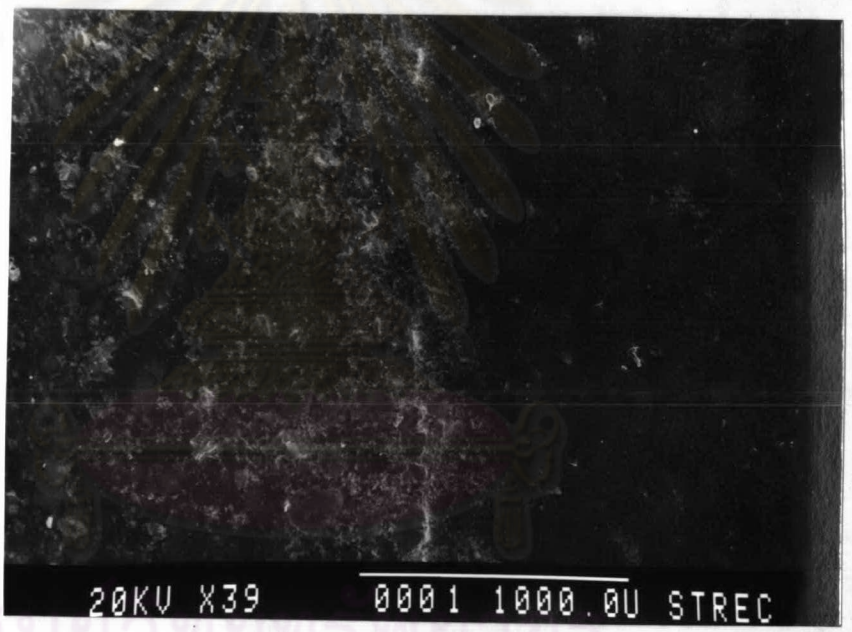

Fig.4.24 Scanning electron micrograph of the interface of precipitate and glass ; the left side shows the precipitated zone and the right side is the glass zone.

4.5 Decomposition of the precipitated compound (copper oxalate)

The decomposition of copper oxalate was studied by thermogravimetry (TGA) and differential thermal analysis (DTA). In the experiments, the atmosphere used was oxygen gas (see Fig. 4.25) or nitrogen gas (see Fig. 4.26). The results show that the atmosphere has a strong effect on the decomposition. The decomposition of copper oxalate was calculated for the following four cases:

case 1 : $CuC_2O_4 \longrightarrow CuO + CO_2 + CO$;

wt. loss = 47.5 %

case 2 : $CuC_2O_4 \longrightarrow CuO + 2CO$;

wt. loss = 37.0 %

case 3 : $CuC_2O_4 \longrightarrow CuCO_3 + CO$;

wt. loss = 18.5 %

case 4 : $CuC_2O_4 \longrightarrow \frac{1}{2}Cu_2O + \frac{3}{2}CO_2 + \frac{1}{2}CO$;

wt. loss = 52.8 %

The result from TGA vs. DTA curves in Fig. 4.25 and Fig. 4.26 shows that copper oxalate decomposed at approximately 300 - 400 °C. From the weight loss (51.5 %) in the experiments, we conclude that the copper oxalate is decomposed to Cu(I) oxide (case 4). A consecutive re-oxidation (partial) to Cu(II) leads to a weight gain of 8.5 %. At the peak at 1069.6 °C (Fig. 4.25, O_2 atmosphere), the Cu_2O forms a eutectic melt in the sub-system Cu_2O-CuO

DATE	: 20 Mar 1995
TIME	: 12:54:39
PROJECT I.D.	: CuC204
TEST I.D.	: N6
SAMPLE	: 001
REFERENCE	: ALZD3
HEATING RATE	: 10
TEMP RANGE	: 20/1200
ATMOSPHERE	: AIR
FLOW RATE	: 207 ml/min
INSTRUMENT	: NETZSCH STA 409 C

DESCRIPTION		SAMPLE	REFERENCE
WEIGHT	mg	103.6	99.8

CHANNEL	RANGE	RAW	COR.
TEMPERATURE	4000	X	
MASS	500	X	
DSC	500	X	

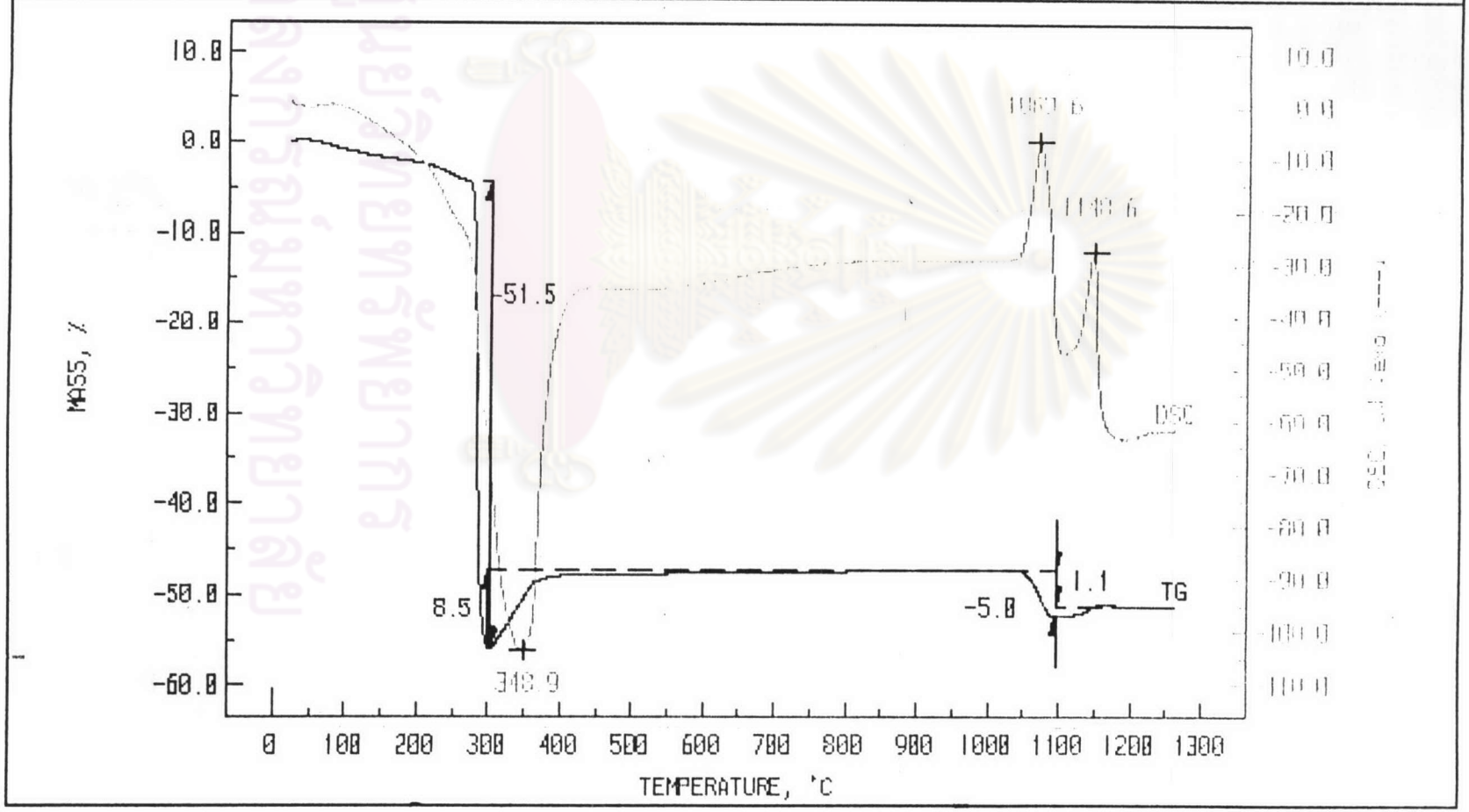

Fig. 4.25 TGA VS. DTA curve of CuC_2O_4 in O_2 gas atmosphere

DATE	: 20 Mar 1995
TINE	: 17:10:41
PROJECT I.D.	: CuC204
TEST I.D.	: N7
SANPLE	: 002
REFERENCE	: AL2D3
HEATING RATE	: 10
TENP RANGE	: 20/1200
ATNOSPHERE	: N2
FLOW RATE	: 207
INSTRUNENT	: NETZSCH STA 409 C

DESCRIPTION		SAMPLE	REFERENCE
WEIGHT	mg	99.2	99.4

CHANNEL	RANGE	RAW	COR.
TEMPERATURE	4000	X	
MASS	500	X	
DSC	500	X	

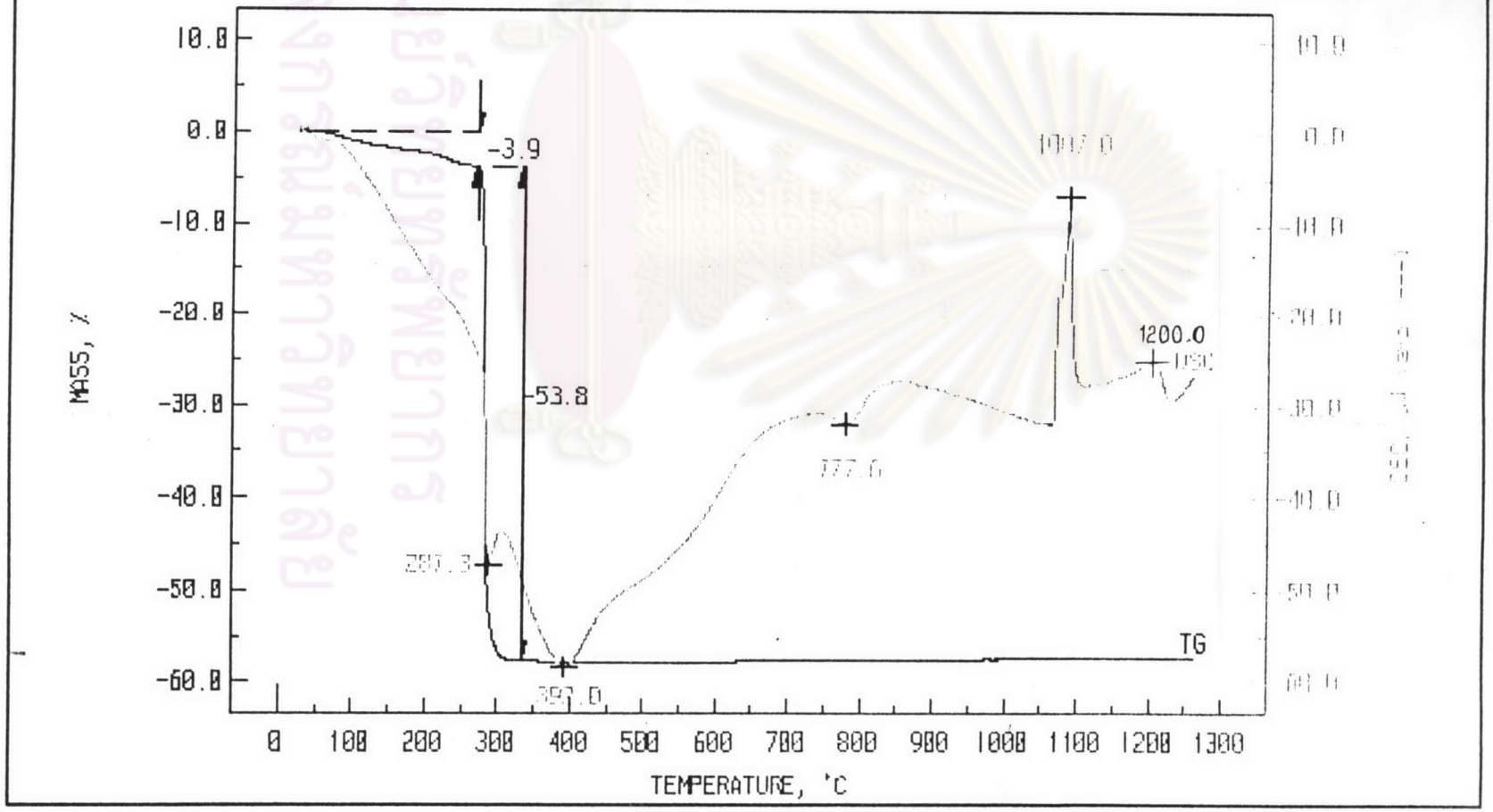

Fig. 4.26 TGA VS. DTA curve of CuC_2O_4 in N_2 gas atmosphere

(see right side of the Cu-O phase diagram in appendix A(A)). At the peak at 1087.0 °C (Fig. 4.26, N_2 atmosphere), the Cu_2O forms a eutectic melting the sub-system Cu-Cu_2O (see left of the Cu-O phase diagram in appendix A(A)). The peak at 1200 °C is the reaction point in the sub-system Cu-Cu_2O. As a long term objective, we want copper in the form of metallic copper. So the oxygen partial pressures for the transition CuO ---> Cu_2O and Cu_2O ---> Cu were calculated as a function of temperature by using the constants in appendix C. At temperatures below the sinter temperature (safe range : T < 540 °C), $P(O_2)$ must be kept as low as 10^{-14} bar (see Fig. 4.27). With N_2-H_2 gas mixtures (see Fig. 4.28) this can be achieved in practice. However, care must be taken to stay away from the range where SiO_2 is reduced (see Fig. 4.29). These steps are meant as recommendations to be used in the parallel thesis on sintering.

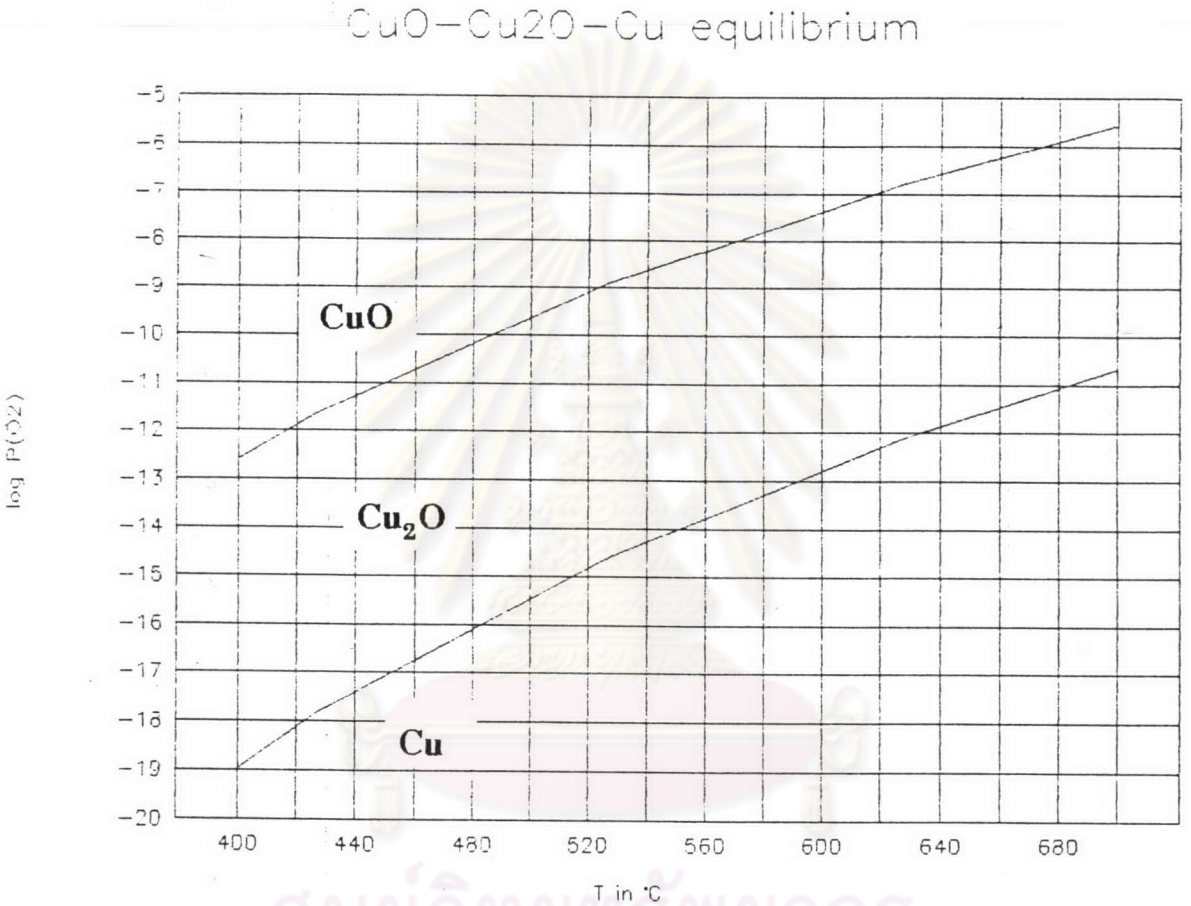

Fig. 4.27 Oxygen partial pressures for the transition CuO --> Cu_2O and Cu_2O --> Cu VS. temperature

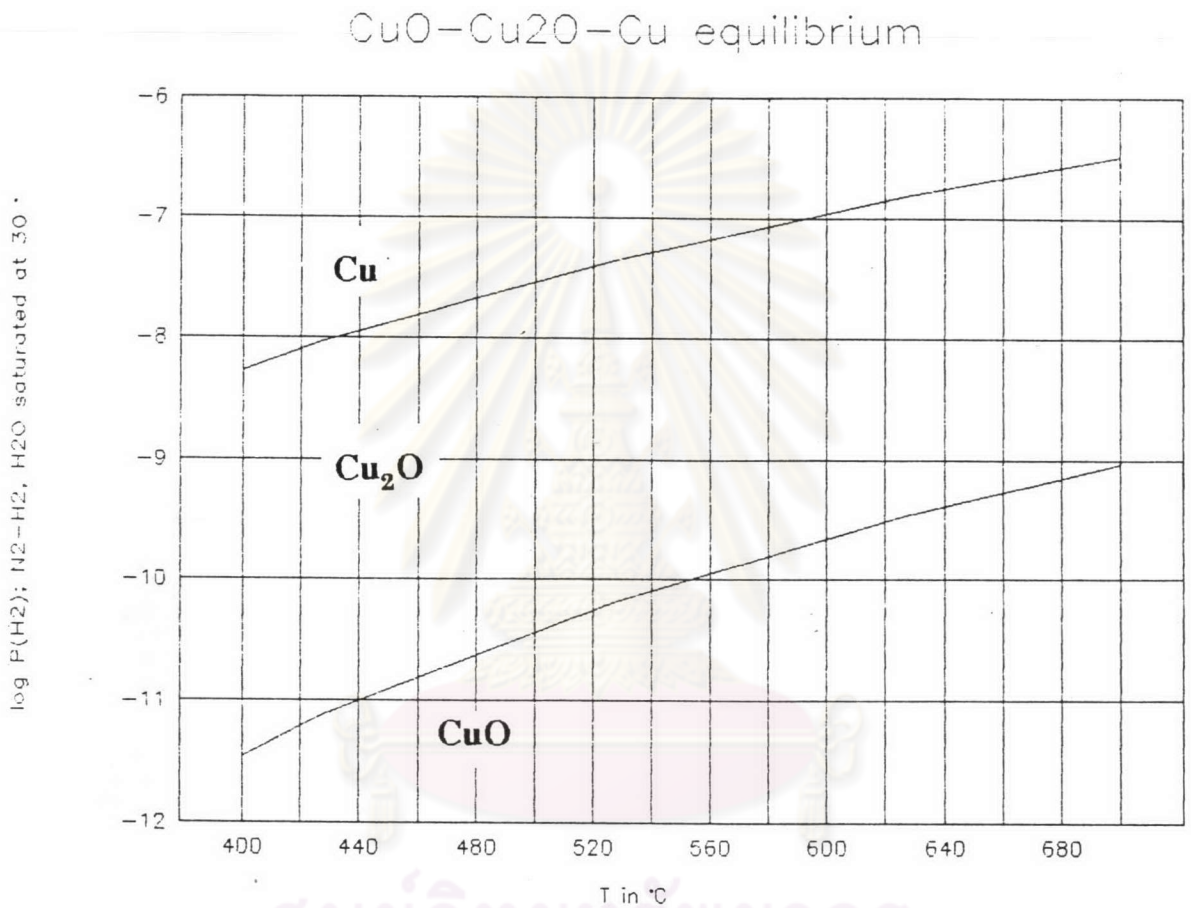

Fig. 4.28 Hydrogen partial pressures for the transition CuO --> Cu_2O and Cu_2O --> Cu VS. temperature

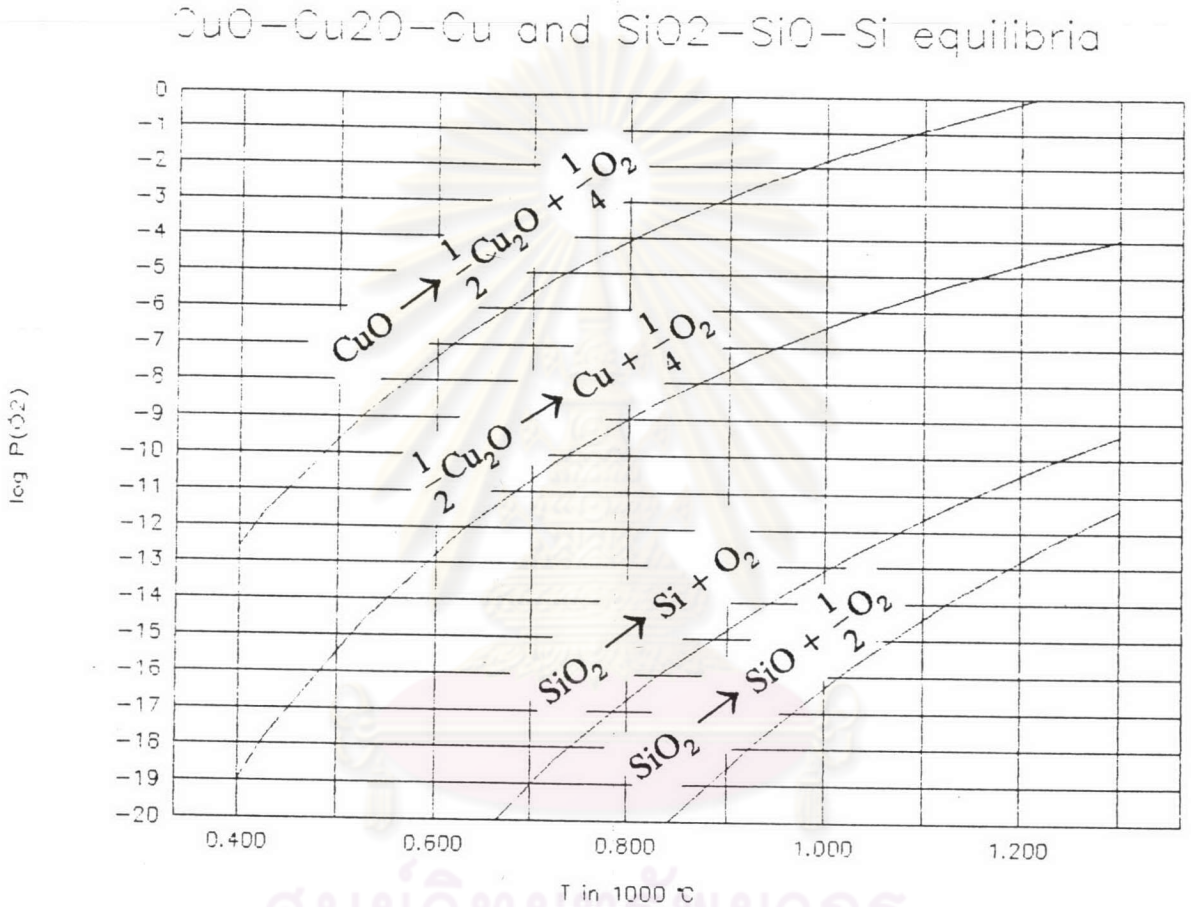

Fig. 4.29 Oxygen partial pressures for the transition CuO --> Cu_2O and Cu_2O --> Cu, compare with the transition SiO_2 --> Si and SiO_2 --> SiO VS. temperature